RESEARCH ARTICLE

Amyloid detection and typing yield of skin biopsy in systemic amyloidosis and polyneuropathy

Sandra Pinton[1,2], Elena Vacchi[1,2,3], Giacomo Chiaro[1,2], Andrea Raimondi[4,5], Alexandar Tzankov[6], Bernhard Gerber[7,8], Claudio Gobbi[1,3], Alain Kaelin-Lang[1,2,3,9] & Giorgia Melli[1,2,3] (iD)

[1]Neurology Department, Neurocenter of Southern Switzerland, Ente Ospedaliero Cantonale, Lugano, Switzerland
[2]Neurodegenerative disorders lab, Laboratories for Translational Research, Ente Ospedaliero Cantonale, Bellinzona, Switzerland
[3]Faculty of Biomedical Sciences, Università della Svizzera Italiana, Lugano, Switzerland
[4]Institute for Research in Biomedicine, Università della Svizzera italiana, Bellinzona, Switzerland
[5]Experimental Imaging Centre, IRCCS San Raffaele Scientific Institute, Milan, Italy
[6]Histopathology, Institute of Medical Genetics and Pathology, University Hospital Basel, Basel, Switzerland
[7]Clinic of Hematology, Oncology Institute of Southern Switzerland, Ente Ospedaliero Cantonale, Bellinzona, Switzerland
[8]University of Zurich, Zurich, Switzerland
[9]Department of Neurology, Inselspital, Bern University Hospital, University of Bern, Bern, Switzerland

Correspondence
Giorgia Melli, Neurology Department and Neurodegenerative Disorders Lab LRT-EOC, Neurocenter of Southern Switzerland, Lugano, Switzerland. Tel: +41 (0)91 8116535; Fax: +41 (0)91 8116915; E-mail: giorgia.melli@eoc.ch

Abstract

Objective: Disease-modifying therapies are available for amyloidosis but are ineffective if end-organ damage is severe. As small fiber neuropathy is an early and common feature of amyloidosis, we assessed detection and typing yield of skin biopsy for amyloid in patients with confirmed systemic amyloidosis and neuropathic symptoms. **Methods**: In this case–control study, patients with transthyretin and light chain amyloidosis (ATTRv, ATTRwt, and AL) were consecutively recruited. They were sex and age-matched to three control groups (1) non-neuropathic controls (NNC), (2) monoclonal gammopathy of undetermined significance (MGUS), and (3) other neuropathic disease controls (ONC). Patients underwent a double 3 mm skin biopsy in proximal and distal leg. Amyloid index and burden, protein typing by immuno-electron microscopy, intraepidermal nerve fiber density, electroneuromyography, and clinical characteristics were analyzed. **Results**: We studied 15 subjects with confirmed systemic amyloidosis, 20 NNC, 18 MGUS, and 20 ONC. Amyloid was detected in 100% of patients with amyloidosis (87% in ankle and 73% in thigh). It was not detected in any of the control groups. A small fiber neuropathy was encountered in 100% of amyloidosis patients, in 80% of MGUS, and in 78% of ONC. Amyloid burden was higher in ATTRv, followed by AL and ATTRwt. The ultrastructural examination allowed the identification of the precursor protein by immunotyping in most of the cases. **Interpretation**: Skin biopsy is a minimally invasive test with optimal sensitivity for amyloid. It allows amyloid typing by electron microscope to identify the precursor protein. The diagnostic work up of systemic amyloidosis should include a skin biopsy.

Introduction

Long regarded as untreatable and fatal, amyloidosis is a proteinopathy characterized by deposits of extracellular fibrillary misfolded β-sheets aggregates in organs and tissues.[1] To date, 42 amyloidosis-causing precursors have been reported in humans, with immunoglobulin light chain (AL) and transthyretin (ATTR) amyloidosis being the most common ones.[2] Because they are rare and typically manifest with heterogeneous, nonspecific symptoms, AL, and ATTR can be difficult to diagnose, leading to misdiagnosis, and disease progression before amyloid is

detected. Overall, 25% of patients with AL die within 6 months of diagnosis and 25% of patients with ATTR die within 24 months of diagnosis.[3]

AL usually presents with nonspecific symptoms (unexplained sensorimotor neuropathy; autonomic symptoms), whereas the more specific signs, such as macroglossia and periorbital purpura, are quite insensitive.[3,4] A monoclonal plasma cell or B-cell disorder is usually present in the bone marrow biopsy, as is the respective circulating serum precursor protein, usually a monoclonal free light chain. As monoclonal gammopathy of undetermined significance (MGUS) is frequently associated with sensorimotor polyneuropathy, the differential diagnosis with AL neuropathy can be challenging.

The cardiac and peripheral nervous systems are commonly involved in patients with ATTR, both genetic (ATTRv) and sporadic wild type (ATTRwt). ATTRv is caused by a single amino acid substitution produced by a point mutation in the TTR gene. Several mutations are associated with either predominant polyneuropathy or cardiomyopathy; however, most patients experience a mixed phenotype of symptoms.[5–7] ATTR is considered a rare disease, but its prevalence is likely higher than supposed, especially for ATTRwt, whose incidence has increased in the last years, due to growing awareness and improved diagnostics.[8] Recent studies showed that patients with ATTRwt cardiomyopathy also showed a predominately sensory, symmetric polyneuropathy in 74%[9] and a small fiber neuropathy in over 80%.[10]

Due to the recent progresses in RNA-based therapeutic technology, some ATTR subtypes have become treatable.[11] Tafamidis, a kinetic stabilizer of the native tetrameric structure, has been approved for cardiac ATTRwt and ATTRv amyloidosis.[12] More recently, patisiran, a RNA interference (RNAi) agent,[13] and inotersen, an antisense oligonucleotide (ASO),[14] have been approved for ATTRv neuropathy. As none of these drugs target the specific transthyretin mutation,[15] their knockdown efficacy is supposed to work in the far more common ATTRwt as well.[16] Therefore, early diagnosis has gained paramount importance, albeit being far from straightforward, especially in terms of histological confirmation of amyloid.[17,18] Amyloid fibrils may be demonstrated with higher sensitivity from a suspected involved organ, albeit with increased invasiveness (heart, kidney, liver, nerve, and gastrointestinal tract).[19] The abdominal fat aspirate is a widespread procedure with a much higher sensitivity for AL (80%) than for ATTR (12%).[20,21] Moreover, specificity of fat pad aspiration is 93%, underscoring that substantial false positives can occur.[22,23] Other surrogate, but invasive, biopsy sites that can be used for AL are salivary glands (61% sensitivity)[22] and bone marrow (57–70%).[3,24] When amyloid is identified, it is fundamental to characterize the precursor protein, and immune electron microscopy or mass spectroscopy are currently considered the gold standard for amyloid typing.[3]

Skin tissue has been used for amyloid detection, but the size of biopsy, location, and methodological procedure have not been standardized and different, scattered data are available, in most of the cases regarding the abdominal fat pad procedure, which is usually larger in size and requires sutures. The 3-mm punch skin biopsy has obtained increasing attention as a diagnostic tool for ATTRv, mainly because of its little invasiveness and high content in nerve fibers prone to the pathology.[25–27] First, an early skin denervation has been observed in ATTRv, even in the presymptomatic stage of the disease, and intraepidermal nerve fiber density (IENFD) correlated with clinical findings of neuropathy.[28] Second, cutaneous amyloid was identified in 80–86% of ATTRv-neuropathy and 14% of asymptomatic carriers according to two recent studies.[29,30] Further, recent works report that polyneuropathic symptoms are common presenting features across several TTR variants, including those that are considered mainly cardiac like V122I.[31] Scant if any data are available on amyloid detection in skin biopsy of patients with ATTRwt and AL, who frequently present with a sensory polyneuropathy. Further 3-mm punch skin biopsy has never been exploited for amyloid typing. In this study, we assessed the diagnostic yield of skin biopsy for amyloid deposits, including electron microscope immunotyping, in consecutive patients with systemic amyloidosis (sAML) and symptoms of peripheral neuropathy.

Materials and methods

Patient recruitment and clinical evaluation

In this case–control study, patients with a clinical diagnosis of ATTRv, ATTRwt, and AL, according to published criteria,[3,4] referred to the neuromuscular clinic at the Neurocenter of Southern Switzerland (NSI) for symptoms suggestive of peripheral neuropathy (sensory complaints, or/and pain, or/and imbalance), were recruited consecutively from June 2020 to April 2023. Sex- and age-matched controls were selected among subjects sent for sensory complaints or/and pain with normal electrophysiological tests and normal IENFD by skin biopsy (non-neuropathic controls, NNC) and among patients suffering from non-amyloidotic peripheral neuropathies with positive electrophysiological tests and/or reduced IENFD (other neuropathic controls, ONC). Another control group included patients with MGUS and confirmed polyneuropathy by electromyography and/or skin biopsy. All subjects underwent a standardized assessment, inclusive of history taking and detailed neurological evaluation with total neuropathy

score (TNS),[32] electroneuromyography, and skin biopsy. Blood tests were performed to assess systemic causes of polyneuropathy (glycosylated hemoglobin test [HbA1c], thyroid-stimulating hormone [TSH], vitamin B12 and folate levels, serum protein electrophoresis, antinuclear antibody [ANA], and nuclear antigen antibody [ENA] screening panel, human immunodeficiency virus [HIV], hepatitis C virus [HCV], and Borrelia serologies). All research studies have been performed in accordance with the principles stated in the Declaration of Helsinki.

Skin biopsy

As previously described,[33–35] each subject underwent a double 3-mm-punch skin biopsy at two anatomical sites: 10 cm below the trochanter (thigh) and 10 cm above the lateral malleolus (ankle). Skin samples were fixed overnight in paraformaldehyde-lysine-periodate (PLP) 2% fixative.

Intraepidermal nerve fiber density and TTR staining

At least three nonconsecutive 50 μm-thin tissue sections per localization per patient were incubated overnight with the primary antibody against the panaxonal marker protein gene product 9.5 (PGP9.5; Abcam, Cambridge UK, 1:1000) or anti-TTR Abcam, Cambridge UK). Cell nuclei were counterstained with 4′,6-diamidino-2-phenylindole (DAPI, Sigma-Aldrich, Saint Louis USA, 1:5000). Sections were analyzed with an inverted fluorescence microscope (Nikon Eclipse Ti-E, Tokyo, Japan). The linear IENFD was obtained according to published protocols and expressed as "number of fibers/mm."[36,37] Intensity of staining and percentage of TTR positive structures were semiquantitatively assessed by two investigators in a blinded manner.

Amyloid deposits evaluation and analysis

Congo red staining was performed to visualize amyloid deposits and performed according to published protocols.[25,27,38] A solution with Congo Red (Sigma-Aldrich, Saint Louis USA) 2.5 g in 500 mL of 80% ethanol (Sigma-Aldrich, Saint Louis USA), saturated with 1 g potassium hydroxide (Sigma-Aldrich, Saint Louis USA), pH 11 was prepared and nonconsecutive 50-μm-thin tissue sections, were incubated with it for 45 min. Sections were rinsed in tap water for 5 min, counterstained with Hematoxylin solution (Vector Laboratories, Burlingame, USA) for 2 min, and then washed for 1 min with the differentiating solution: 0.2% hydrochloric acid (Sigma-Aldrich, Saint Louis USA) and 80% ethanol (Sigma-Aldrich, Saint Louis USA). Finally, sections were rinsed in tap water for 10 min, washed in tris-buffered saline (TBS;

ThermoFisher Scientific, Waltham USA) for 10 min, and then mounded with Vectashield mounting medium (Vector Laboratories, Burlingame, USA).

Under light and polarized microscopy (Zeiss Axio Lab.A1 Microscope, AxioCam ERc 5 s, Oberkochen, Germany), skin sections were first rated with brightfield to identify Congo red signals, and then each signal was analyzed with polarized light to visualize the characteristic birefringence, specific for amyloid deposits.[25,27,38,39] Further confirmation of the amyloid nature of the deposits was obtained by screening the birefringent signals also under an inverted fluorescence microscope with a Texas red filter[40–42]: only positive signals showing birefringence with polarized light and a red autofluorescence were considered real amyloid deposits (Fig. 1A).

Photographs of positive sections were taken at 4x magnification with light and polarized microscopy and analyzed with ImageJ software. The amyloid area/dermis area was quantified as "amyloid burden."[25,27]

Sections were defined as "positive" if showing at least one amyloid deposit. Ankle and thigh were defined as "positive" when at least one positive section was present. The subjects were defined as "positive" when they showed at least one positive site. Negative subjects did not present amyloid signals at any location. For each patient and localization, we reported the amyloid index, defined as the number of sections positive for amyloid deposits divided by the total number of sections examined,[27] the number of amyloid signals per section, the distribution of the amyloid deposits, and the amyloid burden.[25,27]

Electron and immuno-electron microscopy

Unprocessed or Congo red stained 50-μm-thin tissue sections cryostat sections were fixed for 1 h at room temperature with 2.5% glutaraldehyde in 0.1 M cacodylate buffer pH 7.4, postfixed with reducOned osmium solution (1% OsO4, 1.5% potassium ferrocyanide in 0.1 M cacodylate buffer pH 7.4) for 2 h on ice. After several washes in milli-Q water sections were incubated in 0.5% uranyl acetate overnight at 4°C. Samples were then dehydrated with increasing concentrations of ethanol embedded in epoxy resin and polymerized for 48 h at 60°C between two plastic acetate sheets.

Ultrathin sections were obtained using an ultramicrotome (UC7, Leica microsystem, Vienna, Austria), collected on copper or nickel grids, stained with uranyl acetate and Sato's lead solutions, and observed in a Transmission Electron Microscope Talos L120C (FEI, Thermo Fisher Scientific) operating at 120 kV.

Immunoelectron microscopy for amyloid proteins was performed as previously described.[43] Briefly resin sections collected on nickel grids were immersed in 10% H2O2
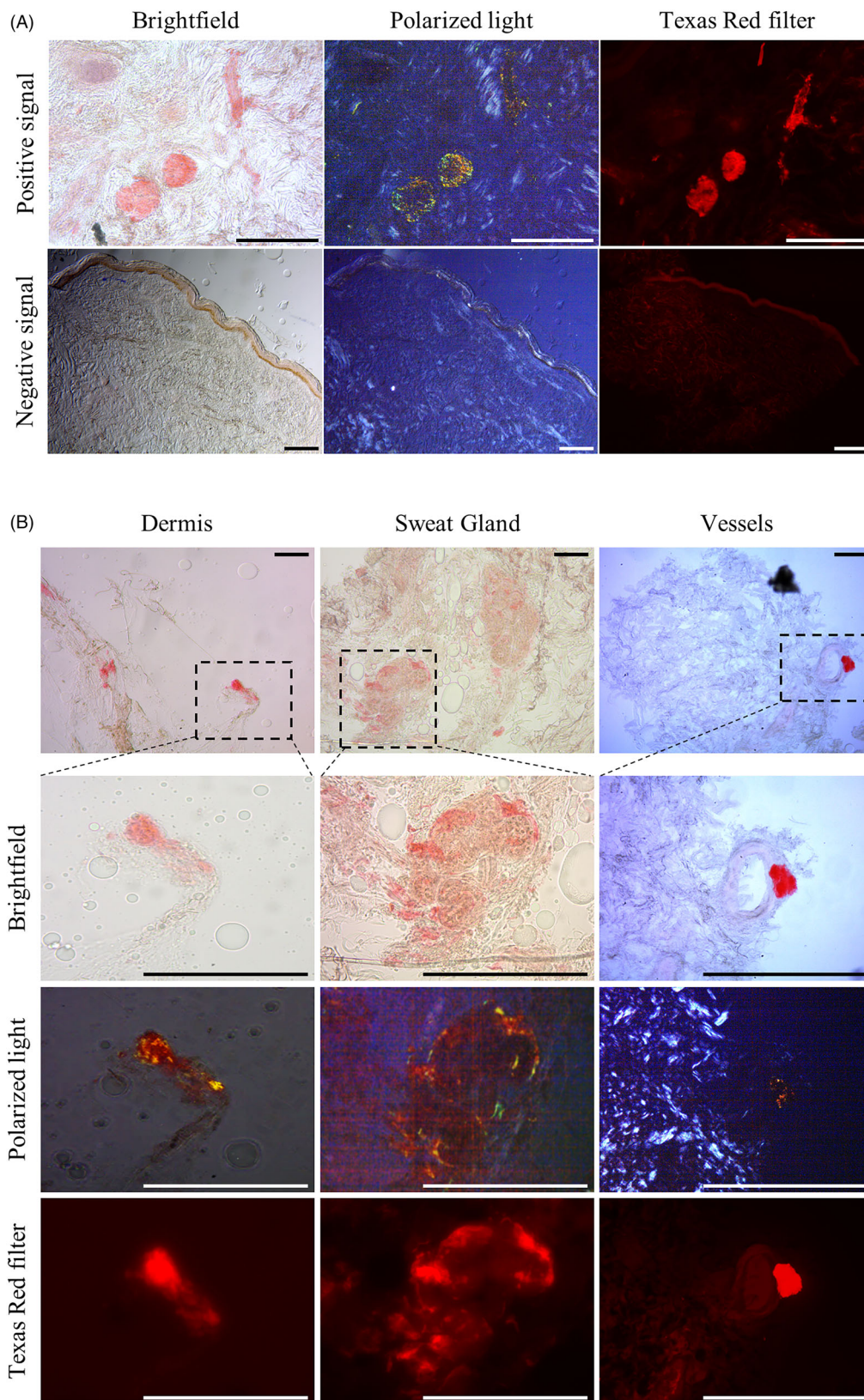
Figure 1. Amyloid signal in skin biopsy. (A) Images of ankle skin sections of ATTRv (top) and NNC (bottom) at brightfield, polarized, and fluorescent microscopy. Congo red deposits in sweat glands present the characteristic birefringence under polarized light and red autofluorescence under Texas red-filtered light. (B) Signals in the deep dermis (left), sweat glands (middle) in ankle skin biopsy of a patient with ATTRwt, and in a vessel (right) in ankle skin biopsy of a patient with ATTRv. Magnifications of inserts are shown. Scale bar 200 μm.

for 5 min at room temperature, washed with distilled water and nonspecific binding was blocked with Aurion blocking solution for 10 min. Grids were then incubated with anti-TTR 1:50 or anti-ALλ 1:50 (AmYmed, München, Germany) diluted in 1% BSA in PBS overnight in a humidified chamber. Grids were washed in PBS (3 × 10min) and incubated with 10 nm gold conjugated secondary antibodies (1:30 Aurion) diluted in PBS/BSA for 30 min. Grids were rinsed six times in milli-Q water and contrasted with uranyl acetate and Sato's lead solutions and observed in a Transmission Electron Microscope Talos L120C (FEI, Thermo Fisher Scientific) operating at 120 kV, by a qualified rater blinded to clinical diagnosis. A signal was considered positive when the antibody bound to amyloid fibrils.

Statistical analysis

Statistical analyses were performed with IBM SPSS Statistics 26.0 (IBM Corp. Released 2020. IBM SPSS Statistics for Windows, Version 26.0. Armonk, NY: IBM Corp). The Kolmogorov–Smirnov test assessed variable distribution. Normally distributed variables (age) were expressed as mean ± standard deviation and analyzed with a one-way ANOVA test with post hoc Bonferroni's test for multiple comparisons. Non-normally distributed variables (Disease Duration, IENFD, TNS) were expressed as medians and interquartile range and analyzed with Kruskal–Wallis' test. Categorical variables were expressed as a percentage (%) and analyzed with chi-squared or Fisher's exact tests.

Results

Clinical characteristics

We analyzed 15 sAML, 20 NNC, 18 MGUS, and 20 ONC based on clinical presentation and diagnostic workup. Demographics and clinical characteristics of groups are summarized in Table 1. In sAML, three were diagnosed

Table 1. Demographic and clinical data.

	sAML (n = 15)	MGUS (n = 18)	ONC (n = 20)	NNC (n = 20)	Overall p-value	sAML vs. MGUS	sAML vs. ONC	sAML vs. NNC
Age (years)	73 ± 14	74 ± 8	71 ± 6	71 ± 14	0.131	–	–	–
Sex (M)	73.3%	66.7%	70.0%	60.0%	0.850	–	–	–
Disease duration (years)	2.5 [1.4–4.5]	1.8 [0.9–5.4]	1.7 [1.0–4.0]	1.1 [0.3–4.3]	0.396	–	–	–
Dysesthesia	93.3%	88.9%	95.0%	100.0%	0.501	–	–	–
Burning pain	6.7%	16.7%	25.0%	30.0%	0.482	–	–	–
Postural Instability	46.7%	33.3%	15.0%	10.0%	**0.047**	0.336	**0.047**	**0.019**
Carpal tunnel	46.7%	11.1%	10.0%	5.0%	**0.005**	**0.029**	**0.019**	**0.006**
Diabetes	6.7%	16.7%	40.0%	20.0%	0.103	–	–	–
Monoclonal gammopathy	46.7%	100.0%	0.0%	0.0%	**0.000**	**0.000**	**0.001**	**0.001**
TNS	11.0 [7.0–16.5]	11.5 [5.5–19.8]	11.5 [6.8–19.8]	8.0 [6.0–10.0]	0.063	–	–	–
LFN	66.7%	61.1%	45.0%	0.0%	**0.000**	0.514	0.111	**0.000**
SFN	100.0%	77.8%	80.0%	0.0%	**0.000**	0.075	0.174	**0.000**
IENFD (no. of fibers/mm) Ankle	2.7 [0.7–5.7]	5.8 [2.4–8.0]	5.8 [4.7–6.9]	11.8 [9.3–12.4]	**0.000**	**0.033**	**0.009**	**0.000**
IENFD (no. of fibers/mm) Thigh	5.2 [2.1–9.1]	5.8 [4.3–10.1]	9.7 [6.9–11.0]	13.1 [10.0–15.5]	**0.000**	0.229	**0.002**	**0.000**

Data are presented as mean ± standard deviation, median [interquartile range], and absolute number (%), as appropriate. p values <0.05 were considered significant and shown in bold.
IENFD, intraepidermal nerve fiber density; LFN, large fiber neuropathy; MGUS, monoclonal gammopathy of undetermined significance; NNC, non-neuropathic controls; ONC, other neuropathic controls; sAML, systemic amyloidosis patients; SFN, small fiber neuropathy; TNS, total neuropathy score.

with ATTRv (Val50Met in two cases and Phe84Ser), six with ATTRwt, and six with AL (five ALλ, one ALκ) (Table 2). A detailed description of clinical information of each subject with sAML is provided in Table S1. The ONC group included six patients with diabetic polyneuropathy, three with chronic inflammatory demyelinating polyneuropathy, one with chemotherapy-associated polyneuropathy, one with hereditary neuropathy with pressure palsies (HNPP), one with low B12 vitamin, and nine with idiopathic polyneuropathy.

While no significant variation was observed in neuropathy severity score, burning pain and sensory symptoms among groups, postural instability, and carpal tunnel syndrome were reported more frequently in sAML than in the other groups. In sAML group, ATTR wt were older than ATTRv and AL, had less severe neuropathy, and presented more frequently with lumbar stenosis.

Electroneuromyography and skin biopsy

A small fiber neuropathy was encountered in all sAML patients, 77.8% of MGUS and 80% of ONC, while a large fiber neuropathy was found in 66.7% of sAML, 61% of MGUS, and 45% of ONC. Specifically, sAML had a significantly lower IEFND at ankle than MGUS and ONC, while sAML and MGUS had similar IENFD at thigh, which was significantly lower than ONC (Table 1). sAML patients showed decreased IENFD at both sites, in a length dependent fashion. ATTRwt presented less frequently with large fiber neuropathy than ATTRv and AL (Table 2).

Amyloid deposits in skin biopsy

Combining both sites, amyloid deposits were detected in 100% of sAML patients independently of the type of amyloidosis: specifically in 87% of ankle and 73% of thigh skin specimens. All subjects with ATTRv and AL were positive in ankle, while 33% of ATTRwt were negative in ankle and positive in thigh or vice versa. ONC, MGUS, and NNC subjects did not present amyloid at any of the two biopsy sites. The minimum number of sections needed to be analyzed to obtain a positive amyloid signal was 30.

The amyloid index was variable, being higher in ATTRv, followed by AL and ATTRwt. The amyloid burden ranged from 0.1% to 14.8%, being generally greater in ankle than thigh, higher in ATTRv group with 8% in ankle and 2.6% in thigh, followed by AL with 0.8% in both ankle and thigh and ATTRwt with 0.2% in ankle and 0.1% in thigh (Table 2).

Amyloid was detected in the following structures: nerve bundles, vessels, sweat glands, and less frequently in deep dermis in all groups (Fig. 1B). The number of signals for

Table 2. Clinical data and amyloid analysis in systemic amyloidosis subgroups.

	ATTRv (n = 3)	ATTR wt (n = 6)	AL (n = 6)
Clinic			
Age (years)	60 ± 24	83 ± 3	70 ± 10
Sex (% Male)	33.3	100.0	66.7
Disease duration (years)	3.4 [2.5–4.5]	2.2 [1.4–4.3]	2.2 [0.5–8.1]
Burning pain (%)	0.0	16.7	0.0
Dysesthesia (%)	100.0	83.3	100.0
Carpal tunnel syndrome (%)	33.3	83.3	16.7
Lumbar spinal stenosis (%)	0.0	66.7	0.0
TNS	13.0 [9.0–16.0]	8.5 [6.0–28.8]	13.0 [7.5–26.3]
LFN (%)	100.0	33.3	83.3
SFN (%)	100.0	100.0	100.0
Skin biopsy ankle			
AML deposits (%)	100.0	66.7	100.0
AML index (%)	100.0 [18.0–100.0]	8.1 [0.0–56.5]	46.6 [5.9–100.0]
AML burden (%)	7.9 [1.2–14.8]	0.2 [0.0–1.9]	0.8 [0.3–1.9]
No. of signals	81 [68.0–277.0]	4.5 [0.0–17.5]	20.5 [1.8–37.5]
Nerve bundles (%)	26.7 [8.8–44.4]	0.0 [0.0–8.9]	40.2 [5.7–55.3]
Vessels (%)	47.3 [17.7–54.3]	0.0 [0.0–8.9]	15.5 [0.0–49.8]
Sweat gland (%)	23.5 [1.2–73.5]	3.6 [0.0–60.7]	29.4 [0.0–82.7]
Deep dermis (%)	0.0 [0.0–0.0]	0.0 [0.0–94.6]	0.0 [0.0–2.9]
IENFD (no. of fibers/mm)	0.1 [0.0–5.8]	4.4 [2.2–5.6]	1.7 [1.1–6.1]
Skin biopsy thigh			
AML deposits (%)	100.0	66.7	66.7
AML index (%)	100.0 [25.8–100.0]	5.3 [0.0–34.5]	53.3 [0.0–100.0]
AML burden (%)	2.6 [0.9–9.7]	0.1 [0.0–1.2]	0.8 [0.0–2.2]
No. of signals	51.0 [44.0–185.0]	1.0 [0.0–12.8]	25.0 [0.0–66.8]
Nerve bundles (%)	27.0 [18.2–33.3]	0.0 [0.0–2.5]	19.1 [0.0–46.8]
Vessels (%)	48.7 [27.5–50.0]	0.0 [0.0–25.0]	19.9 [0.0–43.7]
Sweat gland (%)	23.8 [17.7–31.8]	45.0 [0.0–100.0]	10.9 [0.0–39.9]
Deep dermis (%)	0.5 [0.0–21.6]	0.0 [0.0–0.0]	0.0 [0.0–0.0]
IENFD (no. of fibers/mm)	6.6 [0.0–9.5]	5.7 [3.7–10.5]	2.6 [2.1–6.9]

Data are presented as mean ± standard deviation, median [interquartile range], and absolute number (%), as appropriate.
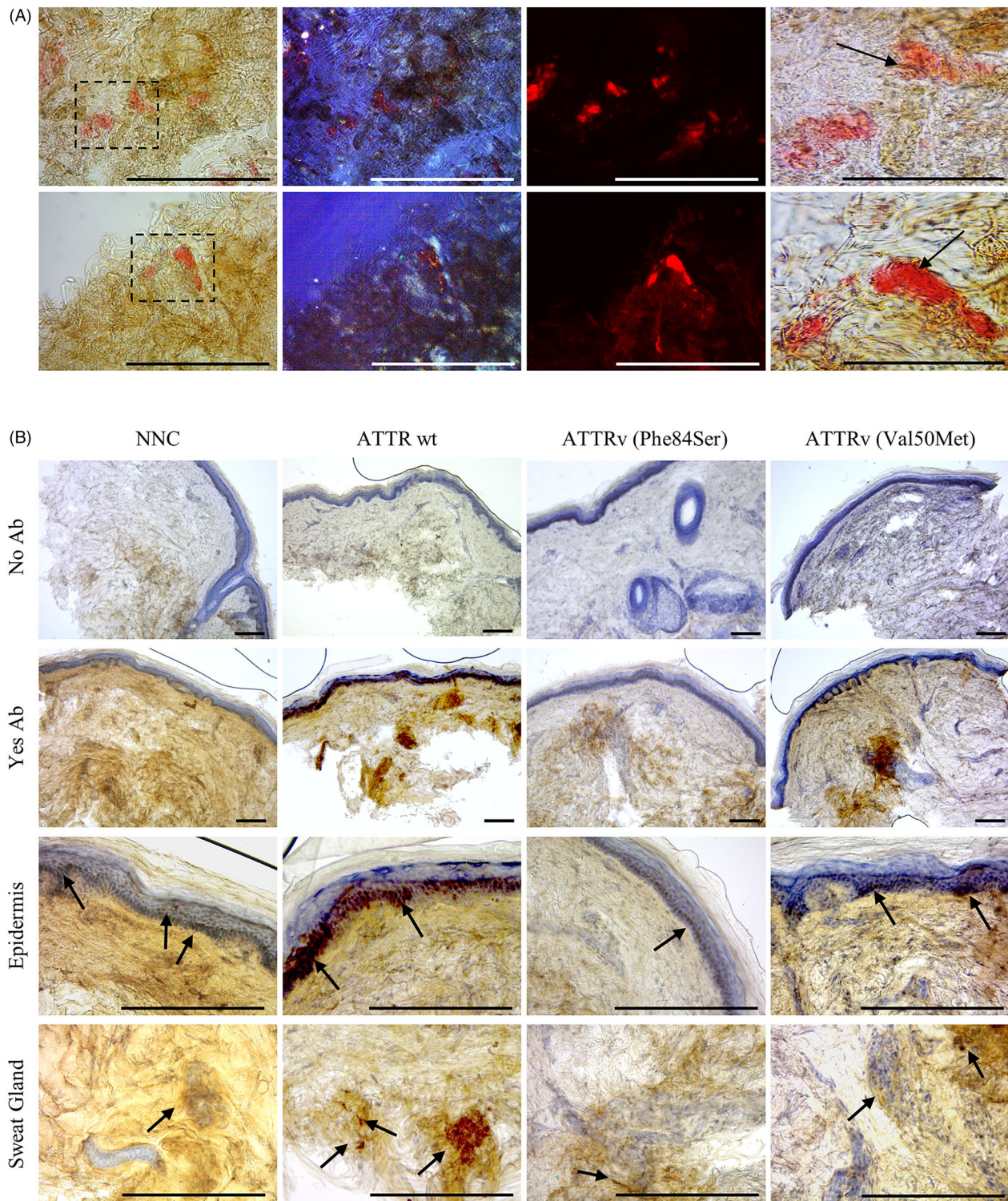
Figure 2. Axonal and TTR immunostaining. (A) Images of ankle skin sections stained with Congo red and anti-PGP9.5 (panaxonal marker) of ATTRwt (upper panel) and AL λ (bottom panel). Amyloid deposits in the deep dermis presented birefringent and autofluorescent signals under polarized and fluorescent microscopy respectively and were in close proximity/infiltrating nerve fibers (arrows). Magnifications of inserts are shown on the left. (B) IHC with anti-TTR showing expression of the protein mainly in epidermis and sub-epidermis in a control subject; a greater expression is noted in epidermis and sweat glands in a ATTRwt subject versus two ATTRv subjects with different mutations. Scale bar 200 μm.

structure and group is reported in Table 2. In general, in ATTRwt amyloid signal was found mainly in sweat glands, in AL mainly around vessels and nerve bundles, in ATTRv in all structures. Of note, the signal was overall more intense at polarized light in ATTRv than ATTRwt. Several amyloid deposits were detected in proximity and infiltrating nerve fibers and bundles in the dermis and around sweat glands, as shown by counterstaining skin sections positive for amyloid with PGP9.5 antibody as axonal marker (Fig. 2A).

Transthyretin expression in skin

Anti-TTR staining showed the protein in epidermis and sweat glands in all subjects including control subjects and sAML patients. In particular, the quantification of TTR-positive sweat glands in a subset of patients (three NNC, two ATTRwt, and two ATTRv) showed similar expression in NNC and ATTRwt treated with tafamidis while a lower expression was observed in ATTRv treated with patisiran (Fig. 2B).

Amyloid ultrastructural analysis and typing by electron microscopy

In skin sections amyloid deposits analyzed by TEM, appeared as randomly oriented, non-branching fibrils of variable diameter and length, independently from the precursor protein. In ATTRwt patients, fibrils displayed a different morphology characterized by longer, sparser structures than ATTRv and AL (Fig. 3). By immune-labeling with anti-TTR we observed a strong positivity of fibrils in ATTRv cases, and a milder positivity in two out of four ATTRwt. By immunostaining with anti-ALλ, we observed a strong positivity in all the ALλ cases and a negative staining in the ALκ case (Fig. 4).

Discussion

In this work, we demonstrated that skin biopsy is an optimal diagnostic tool for detecting and typing amyloid deposits in patients with systemic amyloidosis presenting symptoms of polyneuropathy. In the first place, the combination of two 3 mm-punch skin biopsies performed at the distal leg and thigh showed 100% sensitivity and

specificity in identifying amyloid aggregates by Congo red staining in sAML, independently by the precursor protein. Second, the skin biopsy assay allows the immunotyping of the precursor protein by electron microscope providing a prompt diagnosis and swift access to effective treatments. These findings are of relevance because disease-modifying therapies for sAML are effective only if started at early, less severe stages and sAML are often underdiagnosed.

To our knowledge, this is the highest diagnostic yield for skin biopsy reported in the literature so far. Whereas several reports showed promising results in terms of amyloid detection in genetic variants of ATTR,[25,27,29,30] any data are available for ATTRwt and AL. In all previous studies, the specificity was 100%. The greater sensitivity of our study is likely explained by the number of sections analyzed per biopsy, which was higher than in previous reports (30 sections in this work versus 8–10 sections in Ebenezer's report,[25] 6 sections in Freeman's[30]). As Congo red staining is an easy, and inexpensive procedure, increasing the number of sections to be analyzed in skin biopsy is recommended to achieve a correct diagnosis. Indeed, it is conceivable in the future to analyze them by a semiautomated system. To date, amyloid target tissues, like sural nerve, and endomyocardial biopsies are the gold standard to diagnose amyloidosis neuropathy and cardiomyopathy respectively, but they are invasive. Surrogate tissues are also used,[44,45] they have shown a sensitivity to detect amyloid varying from 57% to 91%[18] and are more invasive than a 3-mm-skin biopsy. This study demonstrates how skin biopsy has an excellent diagnostic performance, in front of a minimally invasiveness, and can be used in clinical practice not only for ATTRv but also for AL and ATTRwt.

In ATTRwt, skin showed a lower amyloid amount than ATTRv and AL, but a specific pattern of distribution in proximity of sweat glands and the ultrastructural analysis confirmed the presence of a different morphology of fibrils respect to ATTRv, as described in literature.[46] Therefore, in presence of neuropathic symptoms, the sensitivity of skin biopsy is very high for ATTRwt as well, even if presenting with a lower amyloid burden than AL and ATTRv.

Of interest, we did not detect amyloid deposits in the group of other polyneuropathies, and in particular in the MGUS group. Further, patients with MGUS showed a

Figure 3. Amyloid fibrils ultrastructure in amyloidosis subgroups. Diverse amyloid fibrils morphology and structure in several types of sAML in skin sections investigated by TEM. (A) Amyloid fibrils are seen among bundles of collagen fibers and appear as short, fibrils randomly arranged in ALλ; (B) amyloid tight fibrils are localized below smooth muscle cells and surrounded by collagen in ALκ; (C) amyloid fibrils are seen below the basal lamina of epithelial cells and appear longer, sparser and randomly oriented in ATTRwt; (D) amyloid fibrils associated with smooth muscle cells in ATTRv(Phe84Ser); (E) amyloid fibrils localized below smooth muscle cells. in ATTRv(Val50Met).
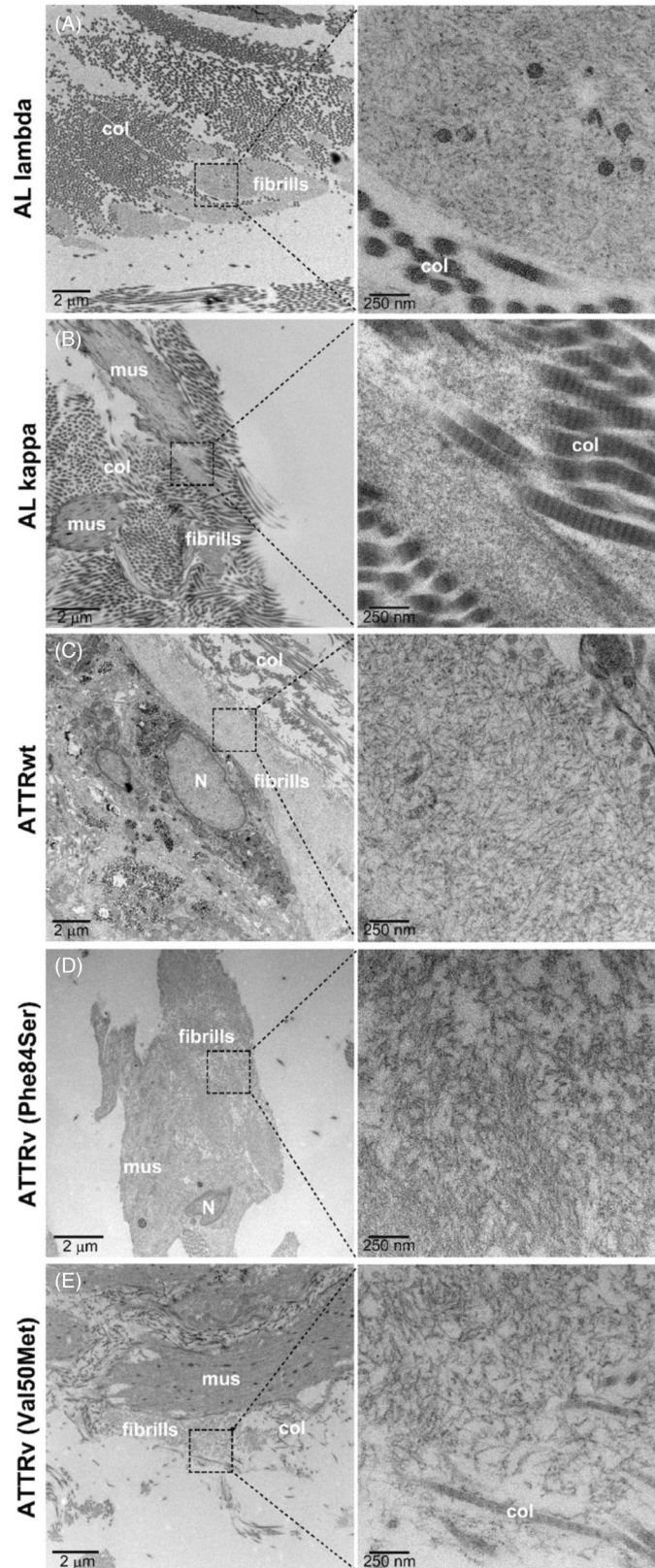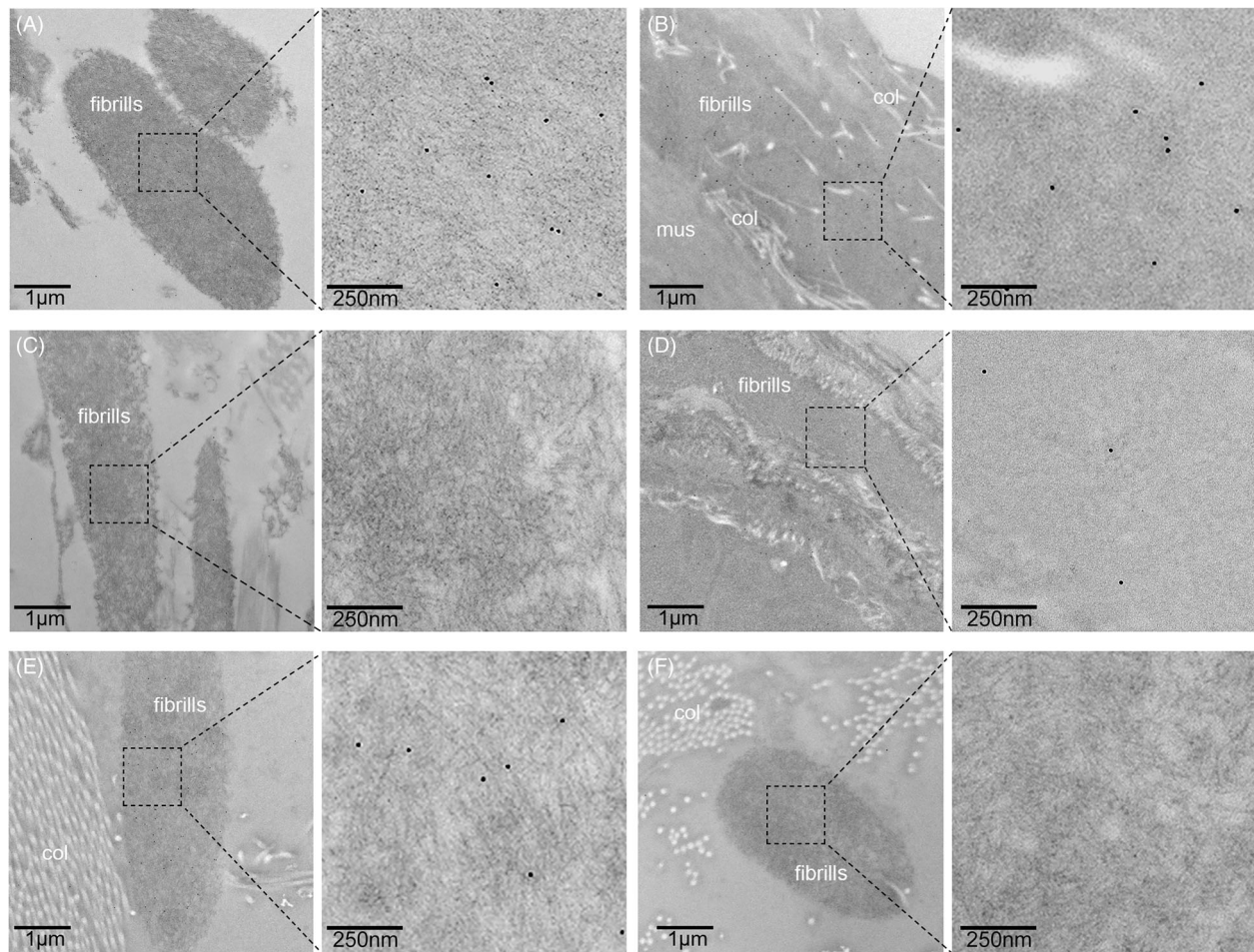
Figure 4. Skin amyloid typing by immuno-electron microscopy. (A) Amyloid fibrils immunostained with anti-TTR in ATTRv(Phe84Ser) and (B) in ATTRv(Val50Met) showing positive signal; (C) amyloid fibrils immunostained with anti-ALλ in ATTRv(Phe84Ser) showing negative signal; (D) amyloid fibrils immunostained with anti-TTR in ATTRwt showing positive signal; (E) amyloid fibrils immunostained with anti-ALλ in ALλ showing positive signal, and (F) with anti-TTR showing negative signal.

non-length dependent small fiber neuropathy, differently from sAML and ONC. As MGUS is frequently associated with peripheral neuropathy in the aging population, skin biopsy can be used to monitor and rule out AL in those cases, where a progression of the disease might raise clinical suspicion of it.

Ultrastructural examination of skin samples allowed the identification of diverse structures and spatial distribution of amyloid fibrils according to the amyloidogenic protein and in ATTRv also according to the TTR mutation. These findings open the intriguing possibility of correlating amyloid fibrils ultrastructure to the heterogeneous clinical phenotypes of patients with ATTR, both genetic and acquired, and AL and can pave the way to the determination of fibril structure for a better understanding of mechanisms of amyloid formation. We used immuno-electron microscopy for amyloid typing, being able to correctly classify all cases of

ATTRv and ALλ and two out of four ATTRwt that were analyzed. These results may be explained by the differential affinity of antibodies for conformational changes of TTR epitopes forming amyloid fibrils. Indeed, by using multiple antibodies directed toward different epitopes it is conceivable to reach a higher performance for correct amyloid typing. Amyloid typing by immuno-electron microscopy is superior to immunohistochemical analysis, which is more challenging and burdened by high rate of false-positive due to unspecific signal.[47] The ultrastructure analysis allows visualization of the amyloid fibrils and with gold-labeled specific antibodies, it can reveal whether the antibodies bind specifically to the amyloid fibrils, or they are unspecifically bound to extracellular proteins outside amyloid structures. Immunoelectron microscopy and laser microdissection followed by tandem mass spectrometry (LMD-MS) are considered gold standards for molecular subtyping

and have shown similar performances in a wide range of tissue biopsies.[48]

TTR protein immunostaining confirmed that it is expressed in skin in physiological conditions, consistent with previous observations,[25] and showed a reduced expression of TTR in skin of ATTRv patients treated with patisiran, a molecule that inhibits the production of mutant and wild-type TTR respect to ATTRwt untreated or treated with tafamidis, a TTR tetramer stabilizer. This raises the possibility to use TTR protein expression in skin biopsy as a target biomarker for testing RNA silencing therapies in clinical trials.

The distribution of amyloid within dermal structures mostly involved autonomic structures, in line with previous findings.[25,27,47] We identified peculiar patterns of distribution according to the amyloid subtype: mainly around sweat glands in ATTRwt, around nerve bundles and vessels in AL, and in all structures in ATTRv.

In all sAML, amyloid deposition was associated with a small fiber neuropathy, independently from the subtype, while a large fiber neuropathy was present in 67%, and specifically only in 33% of ATTRwt. This agrees with previous findings of small fiber neuropathy being present in most cases of ATTR and AL[25,49–50] and with the observation that IENFD reduction is an early event in ATTRv polyneuropathy, presents a stage-dependent progression pattern and precedes amyloid deposition.[27] All together, these results suggest that skin biopsy is more sensitive than electrophysiological studies when precociously assessing a peripheral neuropathy in amyloidosis and that, reasonably, a causal relationship exists between amyloid deposits and nerve damage. The peripheral nerve fiber degeneration in amyloidosis is poorly understood, and several different mechanisms have been considered. The crowding of amyloid around dermal nerve fibers suggests that axonal loss might result from compression and that arteriole involvement accelerates the injury through superimposed ischemia, but different mechanisms affecting different nerve types, or amyloid-inducing axonal injury through oxidative stress must be considered as well.[51]

This study indicates that IENFD and amyloid quantification in skin biopsy are valuable markers to reach a tissue diagnosis of amyloidosis in patients with neuropathic symptoms, and that both markers have a potential role in monitoring disease progression. These findings are of relevance because disease-modifying therapies for ATTR are so far effective only if started at early phases, before end-organ damage has occurred, and presumably do not affect amyloid already present in tissues. In addition to TTR genetic testing, technetium pyrophosphate or methylene diphosphonate scintigraphy of the heart, and sensitive monoclonal protein detection, skin biopsy can play an essential role in the management of patients with amyloidosis.

The main limitations of our work lie in the small size of sAML and the lack of a group of subjects with known amyloidosis, but no symptoms of peripheral nerve involvement. Additionally, more information is needed on the actual prevalence of small fiber neuropathy and sensory neuropathic findings in patients with ATTRwt and a predominant cardiac phenotype.

In conclusion, skin biopsy can change the current diagnostic algorithm for sAML by increasing the sensitivity and specificity of histological confirmation/typing of amyloid in tissue samples in suspected cases of AL and TTR. In front of its low invasiveness, skin biopsy and a neurological assessment should be included also in the diagnostic workup of patients with cardiac phenotypes and suspected ATTRwt or AL.

Acknowledgment

Author Contributions

Sandra Pinton: Acquisition, analysis, interpretation of data and manuscript draft. Elena Vacchi and Giacomo Chiaro: analysis, interpretation of data and manuscript draft. Andrea Raimondi: Acquisition, analysis of data and manuscript revision for intellectual content. Bernard Gerber: patient enrolment, analysis and interpretation of data, revision for intellectual content Alexander Tzankov, Claudio Gobbi and Alain Kaelin-Lang: analysis and interpretation of data, revision for intellectual content Giorgia Melli: Study design, patient enrolment, interpretation of the data, manuscript draft and revision.

Conflict of Interest

The authors report there are no competing interests to declare. BG received fees from Alnylam, Pfizer, Janssen, and an unrestricted research grant from Pfizer, nonrelevant for this article.

Data Availability Statement

Datasets associated with the paper are available from the authors upon reasonable request.

References

1. Koike H, Katsuno M. The ultrastructure of tissue damage by amyloid fibrils. Molecules. 2021;26(15):4611.
2. Buxbaum JN, Dispenzieri A, Eisenberg DS, et al. Amyloid nomenclature 2022: update, novel proteins, and

recommendations by the International Society of Amyloidosis (ISA) nomenclature committee. Amyloid. 2022;29:213-219.

3. Gertz MA, Dispenzieri A. Systemic amyloidosis recognition, prognosis, and therapy: a systematic review. JAMA. 2020;324(1):79-89.

4. Vaxman I, Dispenzieri A, Muchtar E, Gertz M. New developments in diagnosis, risk assessment and management in systemic amyloidosis. Blood Rev. 2020;40:100636.

5. Schwotzer R, Flammer AJ, Gerull S, et al. Expert recommendation from the swiss amyloidosis network (SAN) for systemic AL-amyloidosis. Swiss Med Wkly. 2020;150:w20364.

6. Rapezzi C, Quarta CC, Obici L, et al. Disease profile and differential diagnosis of hereditary transthyretin-related amyloidosis with exclusively cardiac phenotype: an Italian perspective. Eur Heart J. 2013;34(7):520-528.

7. Ando Y, Coelho T, Berk JL, et al. Guideline of transthyretin-related hereditary amyloidosis for clinicians. Orphanet J Rare Dis. 2013;8:31.

8. Nativi-Nicolau JN, Karam C, Khella S, Maurer MS. Screening for ATTR amyloidosis in the clinic: overlapping disorders, misdiagnosis, and multiorgan awareness. Heart Fail Rev. 2021;27(3):785-793.

9. Condoluci A, Théaudin M, Schwotzer R, et al. Management of transthyretin amyloidosis. Swiss Med Wkly. 2021;151:w30053.

10. Kleefeld F et al. Same same, but different? The neurological presentation of wildtype transthyretin (ATTRwt) amyloidosis. Amyloid. 2022 Jan;7:1-10.

11. Papagianni A, Ihne S, Zeller D, Morbach C, Üçeyler N, Sommer C. Clinical and apparative investigation of large and small nerve fiber impairment in mixed cohort of ATTR-amyloidosis: impact on patient management and new insights in wild-type. Amyloid. 2021 Oct;11:1-9.

12. Kole R, Krainer AR, Altman S. RNA therapeutics: beyond RNA interference and antisense oligonucleotides. Nat Rev Drug Discov. 2012;11(2):125-140.

13. Maurer MS, Schwartz JH, Gundapaneni B, et al. Tafamidis treatment for patients with transthyretin amyloid cardiomyopathy. N Engl J Med. 2018;379(11):1007-1016.

14. Adams D, Gonzalez-Duarte A, O'Riordan WD, et al. Patisiran, an RNAi therapeutic, for hereditary transthyretin amyloidosis. N Engl J Med. 2018;379(1):11-21.

15. Benson MD, Waddington-Cruz M, Berk JL, et al. Inotersen treatment for patients with hereditary transthyretin amyloidosis. N Engl J Med. 2018;379(1):22-31.

16. Dohrn MF, Ihne S, Hegenbart U, et al. Targeting transthyretin - mechanism-based treatment approaches and future perspectives in hereditary amyloidosis. J Neurochem. 2021;156(6):802-818.

17. APOLLO-B: a study to evaluate patisiran in participants with transthyretin amyloidosis with cardiomyopathy (ATTR amyloidosis with cardiomyopathy). https://clinicaltrials.gov/ct2/show/study/NCT03997383

18. Koike H, Katsuno M. Transthyretin amyloidosis: update on the clinical Spectrum, pathogenesis, and disease-modifying therapies. Neurol Ther. 2020;9(2):317-333.

19. Abe R, Katoh N, Takahashi Y, et al. Distribution of amyloidosis subtypes based on tissue biopsy site - consecutive analysis of 729 patients at a single amyloidosis center in Japan. Pathol Int. 2021;71(1):70-79.

20. Benson MD, Berk JL, Dispenzieri A, et al. Tissue biopsy for the diagnosis of amyloidosis: experience from some centres. Amyloid. 2022;29(1):8-13.

21. Garcia Y, Collins AB, Stone JR. Abdominal fat pad excisional biopsy for the diagnosis and typing of systemic amyloidosis. Hum Pathol. 2018;72:71-79.

22. Quarta CC, Gonzalez-Lopez E, Gilbertson JA, et al. Diagnostic sensitivity of abdominal fat aspiration in cardiac amyloidosis. Eur Heart J. 2017;38(24):1905-1908.

23. Dhingra S, Krishnani N, Kumari N, Pandey R. Evaluation of abdominal fat pad aspiration cytology and grading for detection in systemic amyloidosis. Acta Cytol. 2007 Nov-Dec;51(6):860-864.

24. Kimmich C, Schönland S, Kräker S, et al. Amyloid in bone marrow smears in systemic light-chain amyloidosis. Amyloid. 2017;24(1):52-59.

25. Ebenezer GJ, Liu Y, Judge DP, et al. Cutaneous nerve biomarkers in transthyretin familial amyloid polyneuropathy. Ann Neurol. 2017;82(1):44-56.

26. Kim DH, Zeldenrust SR, Low PA, Dyck PJ. Quantitative sensation and autonomic test abnormalities in transthyretin amyloidosis polyneuropathy. Muscle Nerve. 2009;40(3):363-370.

27. Chao CC, Hsueh HW, Kan HW, et al. Skin nerve pathology: biomarkers of premanifest and manifest amyloid neuropathy. Ann Neurol. 2019;85(4):560-573.

28. Masuda T, Ueda M, Misumi Y, et al. Reduced intraepidermal nerve fibre density in patients with hereditary transthyretin amyloidosis. Amyloid. 2019;26 (sup1):79-80.

29. Leonardi L, Adam C, Beaudonnet G, et al. Skin amyloid deposits and nerve fiber loss as markers of neuropathy onset and progression in hereditary transthyretin amyloidosis. Eur J Neurol. 2022;29(5):1477-1487.

30. Freeman R, Gonzalez-Duarte A, Barroso F, et al. Cutaneous amyloid is a biomarker in early ATTRv neuropathy and progresses across disease stages. Ann Clin Transl Neurol. 2022;9(9):1370-1383.

31. Kaku MC, Bhadola S, Berk J, Sanchorawala V, Connors LH, Lau KHV. Neurological manifestations of hereditary transthyretin amyloidosis: a focus on diagnostic delays. Amyloid. 2022;29(3):184-189.

32. Cornblath DR, Chaudhry V, Carter K, et al. Total neuropathy score: validation and reliability study. Neurology. 1999;53(8):1660-1664.

33. Vacchi E, Senese C, Chiaro G, et al. Alpha-synuclein oligomers and small nerve fiber pathology in skin are potential biomarkers of Parkinson's disease. NPJ Parkinsons Dis. 2021;7(1):119.

34. Vacchi E, Pinton S, Kaelin-Lang A, Melli G. Targeting alpha synuclein aggregates in cutaneous peripheral nerve fibers by free-floating immunofluorescence assay. J Vis Exp. 2019;(148).

35. Melli G, Vacchi E, Biemmi V, et al. Cervical skin denervation associates with alpha-synuclein aggregates in Parkinson disease. Ann Clin Transl Neurol. 2018;5 (11):1394-1407.

36. Lauria G, Cornblath DR, Johansson O, et al. EFNS guidelines on the use of skin biopsy in the diagnosis of peripheral neuropathy. Eur J Neurol. 2005;12(10):747-758.

37. Provitera V, Gibbons CH, Wendelschafer-Crabb G, et al. A multi-center, multinational age- and gender-adjusted normative dataset for immunofluorescent intraepidermal nerve fiber density at the distal leg. Eur J Neurol. 2016;23 (2):333-338.

38. Menter T, Bachmann M, Grieshaber S, Tzankov A. A more accurate approach to amyloid detection and subtyping: combining in situ Congo red staining and immunohistochemistry. Pathobiology. 2017;84(1):49-55.

39. Howie AJ, Brewer DB, Howell D, Jones AP. Physical basis of colors seen in Congo red-stained amyloid in polarized light. Lab Investig. 2008;88(3):232-242.

40. Fernandez-Flores A. Comparative study of Congo red fluorescence and immunohistochemistry in cutaneous amyloidosis. Romanian J Morphol Embryol. 2010;51 (4):683-686.

41. Marcus A, Sadimin E, Richardson M, Goodell L, Fyfe B. Fluorescence microscopy is superior to polarized microscopy for detecting amyloid deposits in Congo red-stained trephine bone marrow biopsy specimens. Am J Clin Pathol. 2012;138(4):590-593.

42. El-Meanawy A, Mueller C, Iczkowski KA. Improving sensitivity of amyloid detection by Congo red stain by using polarizing microscope and avoiding pitfalls. Diagn Pathol. 2019;14(1):57.

43. Donini U, Casanova S, Zucchelli P, Linke RP. Immunoelectron microscopic classification of amyloid in renal biopsies. J Histochem Cytochem. 1989;37(7):1101-1106.

44. Adams D, Lozeron P, Lacroix C. Amyloid neuropathies. Curr Opin Neurol. 2012;25(5):564-572.

45. Fernandez de Larrea C et al. A practical approach to the diagnosis of systemic amyloidoses. Blood. 2015;125 (14):2239-2244.

46. Bergström J, Gustavsson Å, Hellman U, et al. Amyloid deposits in transthyretin-derived amyloidosis: cleaved transthyretin is associated with distinct amyloid morphology. J Pathol. 2005;206(2):224-232.

47. Chao CC, Huang CM, Chiang HH, et al. Sudomotor innervation in transthyretin amyloid neuropathy: pathology and functional correlates. Ann Neurol. 2015;78 (2):272-283.

48. Abildgaard N, Rojek AM, Møller HE, et al. Immunoelectron microscopy and mass spectrometry for classification of amyloid deposits. Amyloid. 2020;27(1):59-66.

49. Wajnsztajn Yungher F, Kim A, Boehme A, et al. Peripheral neuropathy symptoms in wild type transthyretin amyloidosis. J Peripher Nerv Syst. 2020;25(3):265-272.

50. Yang NC et al. Clinical presentations and skin denervation in amyloid neuropathy due to transthyretin Ala97Ser. Neurology. 2010;75(6):532-538.

51. Kaku M, Berk JL. Neuropathy associated with systemic amyloidosis. Semin Neurol. 2019;39(5):578-588.

Supporting Information

Additional supporting information may be found online in the Supporting Information section at the end of the article.

Table S1